2.6 An Efficient Dual-Resolution Ensemble Data Assimilation Approach and Tests with the Assimilation of Doppler Radar Data

Jidong Gao[1] and Ming Xue[1,2]
[1]Center for Analysis and Prediction of Storms and [2]School of Meteorology
University of Oklahoma, Norman, OK 73019

1. Introduction

To gain a complete understanding of convective storm dynamics and to initialize storm-resolving numerical weather prediction (NWP) models, a complete description of the three-dimensional (3-D) wind, thermodynamic and microphysical fields is needed. The Doppler weather radar, as the only platform that provides volumetric information at the convective storm scale, only observes radial velocity (V_r) and reflectivity (Z). In recent years, various techniques have been developed for analyzing and retrieving the atmospheric state at the convective scale from Doppler radar data. They range from relatively simple single-Doppler velocity retrieval techniques to the four-dimensional variational (4DVAR) method that employs a full prediction model and its adjoint.

For the purpose of initializing storm-scale NWP models, the 4DVAR method (e.g., Sun and Crook 1997; Gao *et al.* 1998) promises to provide an initial condition that is consistent with the prediction model and is able to effectively use multiple volume scans from radar. However, the need to develop and maintain an adjoint code and the associated high computing requirement have limited 4DVAR assimilations of Doppler radar data to relatively simple applications and model settings. The 4DVAR method appears to also have difficulties in dealing with highly nonlinear discontinuous physical processes which become increasingly important at the convective scale.

Since its first introduction by Evensen (1994), the ensemble Kalman filter (EnKF) technique for data assimilation has received much attention. Rather than solving the equation for the time evolution of the probability density function of model state, the EnKF methods apply the Monte Carlo method to estimate the forecast error statistics. A large ensemble of model states are integrated forward in time using the dynamic equations, the moments of the probability density function are then calculated from this ensemble for different times (Evensen 2003).

Corresponding author address: Dr. Jidong Gao, CAPS, 100 E. Boyd, Norman OK 73019.

Recently, EnKF was applied to the assimilation of simulated Doppler radar data for modeled convective storms (Snyder and Zhang 2003; Zhang *et al.* 2004; Tong and Xue 2005) and of real radar data by Dowell et al. (2004). Very encouraging results are obtained in these studies in retrieving wind, temperature and moisture field for convective storms. Tong and Xue (2005) report on the development of an EnKF system based on a general purpose compressible nonhydrostatic model, and on the application of the system to the assimilation of both radial velocity and reflectivity data from a single Doppler radar. The forecast model involves complex ice microphysics rather simple warm rain microphysics used in earlier studies. The ability of the EnKF scheme in 'recovering' the complete state of the model thunderstorms, including wind, temperature, pressure and all water and ice fields is shown to be excellent.

One of the advantages of EnKF method over 4DVAR is that it can dynamically evolve the background error covariances throughout the assimilation cycles, thereby providing valuable uncertainty information on both analysis and forecast. Recently, Caya et al. (2005) showed that with simulated radar data, the EnKF method can outperform a similarly configured 4DVAR scheme after the first few assimilation cycles. When combined with an existing ensemble forecast system (operational ensemble forecasting system is usually run at a lower resolution compared to the operational deterministic forecast), the EnKF method can provide quality analyses with a relatively small incremental cost compared to a 4DVAR system that requires repeated integrations of the forward prediction model and its adjoint.

Still, the overall computational cost of ensemble-based assimilation methods is significant because of the need for running an ensemble of forecast and analysis of nontrivial sizes (usually a few tens to a few hundreds), especially when high-density data are involved and when the ensemble of all forecasts is run at high resolutions. One of the major sources of errors with the ensemble-based DA methods is the sampling error associated with the limited ensemble size. A larger ensemble helps improve the background error covariance estimation.

With 4DVAR, the incremental method proposed by Courtier et al. (1994) enables the use of the so-called double loops and the use of different resolutions of the forecast model in the 4DVAR minimization procedure. Within such an approach, the forward prediction model is run at a higher spatial resolution that defines the nonlinear trajectory around which the linear tangent and the adjoint models are formulated. To reduce computational cost, the tangent linear and adjoint models are run at a reduced resolution within the inner cost-function minimization loops; as a result, the analysis increment is obtained at this lower resolution (LR) but is up converted (usually through interpolation) and added to the high-resolution (HR) forecast background to obtain a single HR analysis. This analysis serves as the initial condition for the HR forecast. It was the cost saving associated with such an incremental procedure that made the operational implementations of 4DVAR practical, and such a procedure is employed in all of today's operational 4DVAR systems.

In this paper, we propose a dual-resolution (DR) hybrid ensemble DA strategy that is in a way analogous to the incremental 4DVAR approach, with the primary goal of reducing the computational cost of the overall EnKF analysis while trying to maintain the benefits of the EnKF algorithms. With this strategy, an ensemble of forecasts is run at a lower resolution which provides the background error covariance estimation for both an ensemble of LR analyses and a single HR analysis. The HR forecast is used to completely replace or partially adjust the ensemble mean of forecast so as to pass the benefit of the HR to the LR ensemble. For storm-scale applications where the grid resolution tends to be marginal at resolving convective storms, the benefit of having a high-resolution component within the DA system can be significant; at the same time, the cross-covariances among the state variables play a key role in 'retrieving' the variables not directly observed by the radar.

We build our DR ensemble DA system based on the ensemble square-root filter (EnSRF) algorithm of Whitaker and Hamil (2002), which is also used by Snyder and Zhang (2003) and Xue et al. (2005). In fact, the implementation follows closely the latter, using the same compressible nonhydrostatic model, the ARPS (Xue et al. 2000; 2003). We test the strategy for the assimilation of simulated radial velocity data, sampled from a simulated supercell storm. The performance of the DR system is compared with the results obtained using a single high resolution (SR).

The rest of this paper is organized as follows. In section 2, we describe our ensemble DA system and the design of the OSS (Observing System Simulation) experiments. The experimental results are presented in section 3. Summary and conclusions are given in section 4.

2. Assimilation System and Experimental Design

a. Hybrid dual-resolution EnSRF algorithm

The basic analysis equation of the Kalman filter is

$$\mathbf{x}^a = \mathbf{x}^f + \mathbf{K}\left[\mathbf{y}^o - H(\mathbf{x}^f)\right]^T, \tag{1}$$

where

$$\mathbf{K} = \mathbf{P}\mathbf{H}^T(\mathbf{R} + \mathbf{H}\mathbf{P}^b\mathbf{H}^T)^{-1} \tag{2}$$

is called the *optimal weighting matrix* (Kalnay 2003) or the Kalman gain matrix. Here, **x** is the state vector we seek to analyze or estimate, and superscripts *a* and *f* refer to the analysis (posteriori estimate) and background forecast (prior estimate), respectively, and $\mathbf{y^o}$ is the observation vector, following the standard notion of Ide et al (1997). *H* is the forward observation operator that maps the model state to the observations, and **H** is the linearized version of *H*. **R** and $\mathbf{P}^b$ are, respectively, the covariance matrices for the observation and background errors.

The key to the ensemble-based filter algorithms is the estimation of the background error covariance and the calculation of the Kalman gain matrix using a forecast ensemble. It was first proposed by Evensen (1994). Since then, there have been a number of further developments with the algorithm to ensure that the technique works when the ensemble size is relatively small (Burgers *et al.* 1998; Houtekamer and Mitchell 1998). Whitaker and Hamil (2002) proposed an ensemble square-root filter algorithm (EnSRF) that does not require the perturbation of observations; the assumption that the observational errors are uncorrelated enables the processing of the observations serially, one at a time, leading to a considerable simplification of the analysis scheme.

As with all Kalman filter algorithms, the EnSRF algorithm proceeds in two steps, an analysis step and a forecast or propagation step. In the analysis step, the following equations are used to update the state vectors for the ensemble mean and individual ensemble members:

$$\overline{\mathbf{x}}^a = \overline{\mathbf{x}}^b + \mathbf{K}\left[\mathbf{y}^o - H\left(\overline{\mathbf{x}}^f\right)\right], \tag{3}$$

$$\mathbf{x}_n^a = \overline{\mathbf{x}}^a + \beta(\mathbf{I} - \alpha\mathbf{K}\mathbf{H})(\mathbf{x}_n^f - \overline{\mathbf{x}}^f), \tag{4}$$

where *n* represents the *n*th ensemble member and the overbar denotes the ensemble mean. β is a covariance inflation factor that is usually slightly larger than 1. The α is given in the EnSRF algorithm by (Whitaker and Hamill 2002)

$$\alpha = \left[1 + \sqrt{\mathbf{R}(\mathbf{H}\mathbf{P}^b\mathbf{H}^T + \mathbf{R})^{-1}}\right]^{-1}. \tag{5}$$

This procedure produces an ensemble of analyses, as given by Eq. (4).

The terms related to the forecast error covariance $\mathbf{P^b}$ are calculated according to

$$\mathbf{P}^b\mathbf{H}^T = \frac{1}{N-1}\sum_{n=1}^{N}\left[[\mathbf{x}_n^b - \overline{\mathbf{x}}^b][H(\mathbf{x}_n^b) - \overline{H(\mathbf{x}^b)}]^T\right] \quad (6)$$

and

$$\mathbf{H}\mathbf{P}^b\mathbf{H}^T = \frac{1}{N-1}\sum_{n=1}^{N}\left[[H(\mathbf{x}_n^b) - \overline{H(\mathbf{x}^b)}][H(\mathbf{x}_n^b) - \overline{H(\mathbf{x}^b)}]^T\right] \quad (7)$$

where N is the number of ensemble members. As can be seen, the nonlinear observation operator H instead of its linearized version $\mathbf{H}$ is used in the equations, removing the approximation associated with linearization.

In the forecast step, forecasts are made from each ensemble analysis and are used as the prior estimate or background in the next analysis-forecast cycle; the algorithm continues as the analysis cycles are repeated.

As discussed earlier, the EnKF or EnSRF algorithms have been successfully applied to the assimilation of single-Doppler radar observations into cloud models (Snyder and Zhang 2003; Zhang et al. 2004; Dowell et al. 2004; Tong and Xue 2005, Xue et al. 2005). The algorithms are, however, expensive, limiting their real-time applications, especially at storm-resolving resolutions over large model domains. For this reason, a more efficient algorithm is proposed here that involves the use of forecast and analysis ensembles produced at a lower resolution plus single analysis and forecast produced at a higher resolution. In this case, the background error covariance is estimated from the lower-resolution ensemble. The specific steps are given below:

1) Integrate a single HR model and an ensemble of LR models forward for the length of the analysis cycle or until the next observation is available, so as to yield a single HR forecast $\mathbf{x}_h^f$ and an ensemble of LR forecasts $\mathbf{x}_n^f$, respectively;
2) Calculate the ensemble mean and ensemble perturbations from the mean from the LR ensemble forecasts according to

$$\overline{\mathbf{x}}^f = N^{-1}\sum_{n=1}^{N}\mathbf{x}_n^f \ , \quad (8)$$

$$\mathbf{x}_n^{'} = \mathbf{x}_n^f - \overline{\mathbf{x}}^f \ . \quad (9)$$

3) Interpolate HR forecast $\mathbf{x}_h^f$ to the LR grid to obtain $\mathbf{x}_{hc}^f$, which is then used to adjust the ensemble mean of the LR forecasts, according to

$$\overline{\mathbf{x}}^f = \alpha\mathbf{x}_{hc}^f + (1-\alpha)\overline{\mathbf{x}}^f \ , \quad (10)$$

where α and (1-α) are the weight coefficients for the HR and the LR ensemble mean forecasts, respectively and the value of α should be between 0 and 1;
4) Use Eqs. (3)-(7) to perform EnSRF analyses serially, one observation at a time; the LR background error covariance is then interpolated to the high resolution grid and used to obtain a HR analysis based on Eqs. (1)-(2);
5) The LR EnSRF analyses and the single HR analysis are used as the initial conditions for the LR ensemble forecasts and for the single HR forecast, respectively. The forecasts are carried out to the next analysis time, from what another analysis and forecast cycle is repeated.

As pointed out earlier in introduction, our proposed dual-resolution hybrid procedure aims to obtain a quality analysis from which high-resolution prediction can be launched, by using background error covariance derived from a cheaper lower-resolution ensemble. For radar data, the covariance contains valuable information on the cross-correlation among different state variables and between the state variables and the radar observed quantities, and such information is key to the 'retrieval' of unobserved state variables. In addition, the ensemble also provides the uncertainty information that a single deterministic forecast cannot provide. In a sense, we attempt to combine the best of both worlds. In fact, a similar strategy has been proposed by Du (2004) in the ensemble forecast context by combining a single high-resolution forecast with a lower-resolution forecast ensemble.

b. Prediction model and truth simulation for OSSEs

In this study, we test our DR hybrid EnSRF algorithm using simulated data from a classic May 20, 1977 Del City, Oklahoma supercell storm (Ray *et al.* 1981). Such simulation experiments are commonly referred to as Observing System Simulation Experiments (OSSE, see, e.g., Lord *et al.* 1997). The prediction model, the ARPS, is used in a 3D cloud model mode and the prognostic variables include three velocity components u, v, w, potential temperature θ, pressure p, and six categories of water substances, *i.e.*, water vapor specific humidity q_v, and mixing ratios for cloud water q_c, rainwater q_r, cloud ice q_i, snow q_s and hail q_h. The microphysical processes are parameterized using the three-category ice scheme of Lin *et al.* (1983). More details on the model can be found in (Xue *et al.* 2000; 2001).

For our experiments, the model domain is 64x64x16 km^2. The LR and HR models have a 2 km and a 1 km horizontal grid spacing, respectively, while the vertical resolution is 500 m in both cases. The truth simulation or nature run is created using the 1 km horizontal resolution and is initialized from a modified real sounding plus a 4 K ellipsoidal thermal bubble centered at x =48, y =16 and z =1.5 km, with radii of 10 km in x and y and 1.5 km in z direction. Open conditions are used at the lateral boundaries. The length of simulation is two hours. A constant wind of u = 3 ms^{-1} and v =14 ms^{-1} is subtracted from the observed sounding to keep

the primary storm cell near the center of model grid. The evolution of the simulated storms is very similar to those documented in Xue *et al.* (2001). During the truth simulation, the initial convective cell strengthens over the first 20 minutes. The strength of the cell then decreases over the next 30 minutes or so, which is associated with the splitting of the cell into two at around 55 minutes (Fig. 1). The right moving (relative to the storm motion vector which is towards north-northeast) cell tends to dominate the system; the updraft reaches a peak value of over 40 ms^{-1} at 90 minutes. The left moving cell starts to split again at 95 minutes. The initial cloud started to form at about 10 minutes, and rainwater formed at about 15 minutes. Ice phase fields appeared at about 20 minutes.

c. Simulation of radar observations

As in Snyder and Zhang (2003) and Tong and Xue (2005), the simulated observations are assumed to be available on the grid points. The simulated radial velocity, V_r, is calculated from

$$V_r = u \sin\phi \cos\theta + v \cos\phi co\,s\,\theta + w \sin\theta \qquad (11)$$

where θ is the elevation angle and ϕ is the azimuth angle of radar beams, and *u, v* and *w* are the model-simulated velocities interpolated to the scalar points of staggered model grid. Random errors drawn from a normal distribution with zero mean and a standard deviation of 1 ms^{-1} are added to the simulated data. Since V_r is sampled directly from velocity fields, the effect of hydrometeor sedimentation is not involved. The ground-based radar is located at the southwest corner of the computational domain, *i.e.*, at the origin of *x-y* coordinate. As with most existing 4DVAR and EnKF studies, the prediction model is also assumed perfect, i.e., no model error is explicitly taken into account.

d. Assimilation experiments

We start the initial ensemble forecast at the 20 minutes of model time when the storm cell developing out of an initial bubble reaches peak intensity. To initialize the ensemble members, random noises are added to the initially horizontally homogeneous background that is based on the environmental sounding. The random noises are sampled from Gaussian distributions with zero mean and standard deviations of 3 m s^{-1} for *u*, *v*, and *w*, and 2 K for potential temperature. These settings are same as Tong and Xue (2005). The pressure, moisture, and microphysical variables are not perturbed at this initial time. The observations are assimilated every 5 minutes. The first analysis is performed at 25 minutes and 40 ensemble members are used. To spatially smooth the analysis increments as well as to localize covariances, Eq. (4.10) of Gaspari and Cohn (1999) is used when calculating the background error matrix $\mathbf{PH}^{\mathbf{T}}$ as suggested by Houtekamer and Mitchell (2001). The weighting coefficient α is set to 0.5.

As an initial effort, we perform two sets of experiments, one using our proposed DR procedure and another using a single high resolution (SR) for the ensemble. For the latter, the algorithm is essentially the same as that used in Xue et al. (2005). Only radial velocity is assimilated in these experiments and the data are assumed to be available in precipitation regions where reflectivity is greater than 10 dBZ.

3. Results of Experiments

This section presents some preliminary results from the OSS experiments described in the previous section. It can seen from Fig. 1 that 5 analysis cycles, by the time of 40 minutes, the basic structures of the updraft and horizontal flow in the DR analysis (Fig. 1e) are reasonably recovered, except for some noise around the main updraft core. The low-level cold pool and the associated flow divergence are still too weak at this time (Fig. 2*e*). By 60 minutes, the strength of the updraft and the magnitude of the potential temperature perturbations become reasonably good (Figs. 1f and 2f), but the left moving cell appears weaker, but the retrieved microphysical fields are rather close to the truth (not shown). By 100 minutes, the low-level flow (Fig. 2h) and reflectivity patterns as well as the shape of the cold pool now agree quite well with the truth (Fig. 2d). The agreement at the 6 km level is even better (Figs. 1h and 1d). These results indicate that even with only the radial velocity data confined to the precipitation regions, our DR assimilation system is able to rebuild the model storm quite well after a sufficient number of assimilation cycles. The lowest panels of Fig. 1 and Fig. 2 show the results of analysis using a single high (1 km) resolution with 40 members. The analyses are notably better than the corresponding DR analyses but the associated computational cost is about twice.

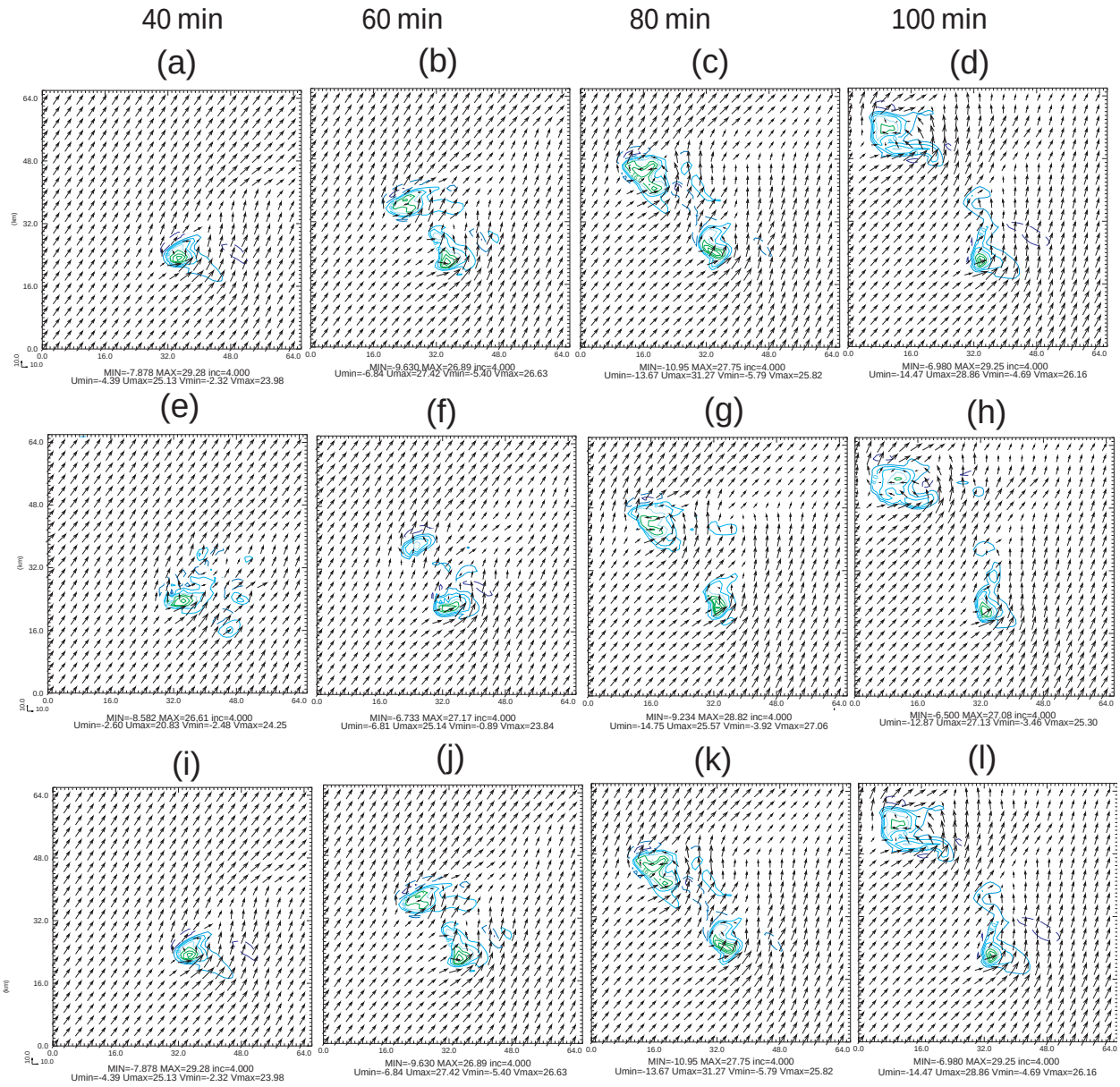

Fig. 1. Vertical velocity w contours, at an interval of 4 ms^{-1}with negative contours dashed, and horizontal wind vectors at 6 km above ground for the truth simulation (a)-(d); ensemble-mean analyses of the dual-resolution hybrid method (e)-(h); and ensemble-mean analyses from the single high-resolution method (i)-(j), at 20, 40, 60 and 80 minutes of model time.

The root-mean-square (*rms*) errors of the analyses using the DR (dashed curves) and SR (solid curves) methods are shown in Fig. 3. The *rms* errors are averaged over those grid points where the reflectivity is greater than 10 dBZ. The *rms* errors of *x*-component of velocity *u*, vertical velocity *w*, perturbation potential temperature θ', water vapor mixing ratio q_v, cloud water q_c and reflectivity *Z* (derived from hydrometer variables rain water, snow and hail) in both experiments are shown to decrease rapidly starting from the time of first analysis (25 min.) during the first five analysis cycles and the analysis errors tend to stabilize at about 50 minutes with both methods. After the analyses stabilize, the *rms* analysis errors for *u* are between 3 and 4 ms^{-1} while those of SR method stay below 2.5 ms^{-1}. The values are similar to *w*. For θ', the analysis errors decrease to less than 1.5 K and 0.5 K respectively at 100 minutes or the end of assimilation window for the two methods (Fig 3c), while the error differences in the water quantities are smaller (Figs. 3d-f). Not surprisingly,

the DR analyses are not as good as those using a single higher resolution, but the algorithm is still able to obtain a quite reasonable estimate of the state of simulated storm, at a significant lower computational cost. The results indicate that the background error covariances obtained from the LR ensemble is still quite effective in the ensemble Kalman filter procedure.

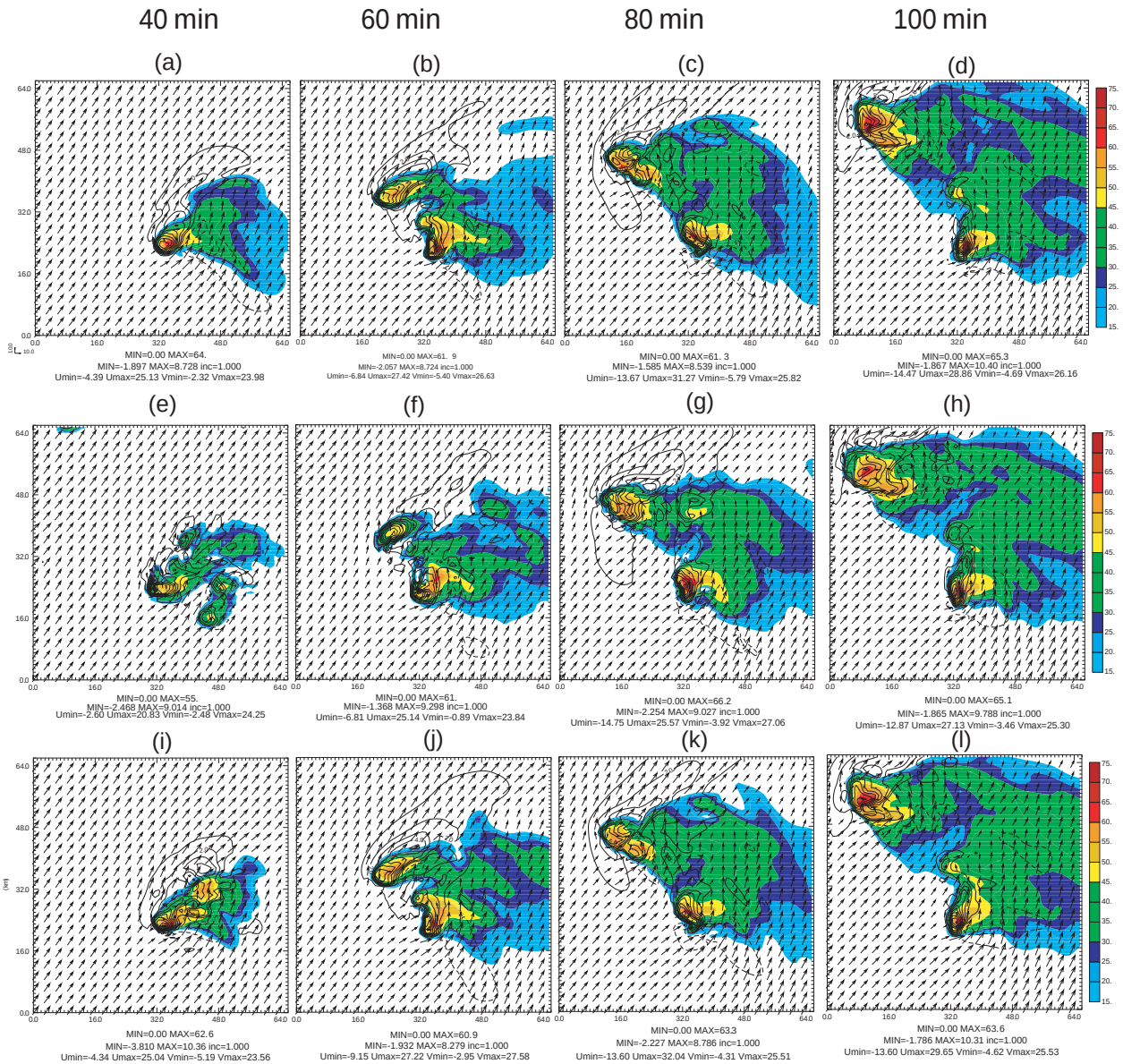

Fig. 2. As Fig. 1, but for horizontal winds (vectors; ms^{-1}), perturbation potential temperature (thick dashed contours at 1 K intervals) and simulated reflectivity (color shaded) at z=250m AGL.

4. Summary and discussion

A new efficient dual-resolution data assimilation algorithm is developed based on the ensemble Kalman filter method and tested with simulated radar data for a supercell storm. Within this algorithm, radar observations are assimilated on both high-resolution and lower resolution grids by using flow-dependent background error covariance estimated from the lower resolution forecast ensemble. The single high-resolution forecast is then used to adjust the ensemble mean of the lower resolution forecasts.

It is shown that the flow-dependent and dynamically evolved background error covariances estimated from the LR ensemble can be effectively used for the assimilation of radar observations. In general, the sys-

tem is able to reestablish the model storm well after a number of assimilation cycles. The DR method has the advantage of a lower computational cost compared to standard ensemble Kalman filter method. The single high-resolution model run may provide valuable small-scale details thereby reducing the impact of resolution-related model errors. The use of a lower-resolution ensemble provides the potential for using a larger ensemble, which may yield a more accurate estimate of the error covariance structure. More experiments are needed to investigate the tradeoffs between accuracy and cost. We will investigate the performance of our procedure for larger resolution ratios in the future, and also evaluate of the quality of forecasts that start from the analyses of various methods.

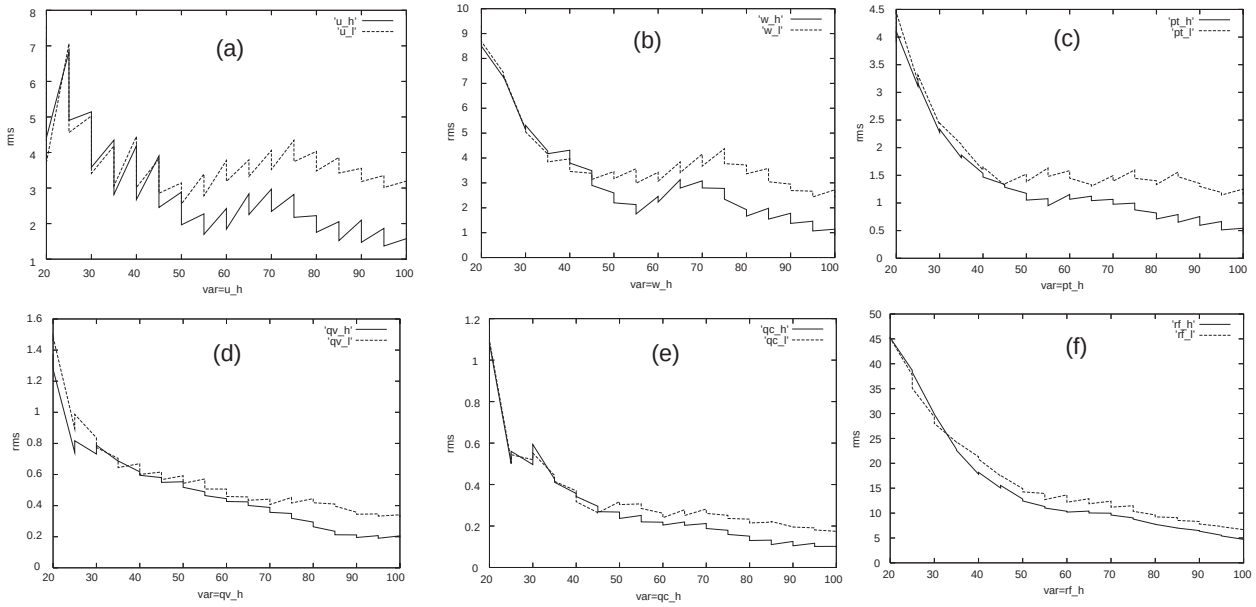

Fig 3: The rms errors of the ensemble mean forecasts and analyses, averaged over points at which the reflectivity is greater than 10 dBZ for: (a) u, (b) w, (c)θ', (d) q_v, (e) q_c, (f) Z for the dual-resolution (dashed) and single high-resolution (solid) experiments.

Acknowledgement

The authors were supported by NSF grants ATM-0331756, ATM-0129892, ATM-0331594 and EEC-0313747, a DOT-FAA grant via DOC-NOAA NA17RJ1227.

References

Anderson, J. L., 2001: An ensemble adjustment Kalman filter for data assimilation. *Mon. Wea. Rev.*, **129,** 2884-2903.

Bishop, C. H., B. J. Etherton, and S. J. Majumdar, 2001: Adaptive sampling with the Ensemble transform Kalman rilter. Part I: Theoretical aspects. *Mon. Wea. Rev.*, **129,** 420.

Burgers, G., P. J. v. Leeuwen, and G. Evensen, 1998: Analysis scheme in the ensemble Kalman filter. *Mon. Wea. Rev.*, **126,** 1719-1724.

Caya, A., J. Sun, and C. Snyder, 2005: A comparison between the 4D-VAR and the ensemble Kalman filter techniques for radar data assimilation. *Mon. Wea. Rev.***,** In press.

Courtier P., J-N Thepaut and A. Hollingsworth 1994: A strategy for operational implementations of 4D-Var, using an incremental approach. *Q. J. Royal Meteorol. Soc.* **120**, 1367-1387.

Dowell, D., F. Zhang, L. J. Wicker, C. Snyder, and N. A. Crook, 2004: Wind and thermodynamic retrievals in the 17 May 1981 Arcadia, Oklahoma supercell: Ensemble Kalman filter experiments. *Mon. Wea. Rev.***,** In press.

Du, J., 2004: Hybrid Ensemble Prediction System: a New Ensembling Approach. Preprints, *Symposium on the 50th Anniversary of Operational Numerical Weather Prediction*, University of Maryland, College Park, Maryland, Amer. Meteor. Soc., CD-ROM.

Evensen, G., 1994: Sequential data assimilation with a nonlinear quasi-geostrophic model using Monte

Carlo methods to forecast error statistics. *J. Geophys. Res.*, **99(C5),** 10143-10162.

——, 2003: The ensemble Kalman filter: Theoretical formulation and practical implementation. *Ocean Dynamics*, **53,** 343-367.

Gao, J., M. Xue, Z. Wang, and K. K. Droegemeier, 1998: The initial condition and explicit prediction of convection using ARPS adjoint and other retrievals methods with WSR-88D data. *12th Conf. Num. Wea. Pred.*, Phoenix AZ, Amer. Meteor. Soc., 176-178.

Gaspari, G. and S. E. Cohn, 1999: Construction of correlation functions in two and three dimensions. *Quart. J. Roy. Meteor. Soc.*, **125,** 723-757.

Houtekamer, P. L. and H. L. Mitchell, 1998: Data assimilation using an ensemble Kalman filter technique. *Mon. Wea. Rev.*, **126,** 796-811.

——, 2001: A sequential ensemble Kalman filter for atmospheric data assimilation. *Mon. Wea. Rev.*, **129,** 123-137.

Ide, K., P. Courtier, M. Ghil, and A. Lorenc, 1997: Unified notation for data assimilation: Operational, sequential and variational. *J. Meteor. Soc. Japan*, **75,** 181-189.

Kalnay, E., 2003: Atmospheric modeling, data assimilation and predictability. Cambridge University Press, Cambridge, 341 pp.

Lin, Y.-L., R. D. Farley, and H. D. Orville, 1983: Bulk parameterization of the snow field in a cloud model. *J. Climate Appl. Meteor.*, **22,** 1065-1092.

Lord, S. J., E. Kalnay, R. Daley, G. D. Emmitt, and R. Atlas, 1997: Using OSSEs in the design of the future generation of integrated observing systems. *Preprint volume, 1st Symposium on Integrated Observation Systems*, Long Beach, CA, Amer. Meteor. Soc.

Hamill, T. M., and C. Snyder, 2000: A hybrid ensemble Kalman filter/3D-variational analysis scheme. *Mon. Wea. Rev.*, **128**, 2905–2919.

Ray, P. S., B. Johnson, K. W. Johnson, J. S. Bradberry, J. J. Stephens, K. K. Wagner, R. B. Wilhelmson, and J. B. Klemp, 1981: The morphology of severe tornadic storms on 20 May 1977. *J. Atmos. Sci.*, **38,** 1643-1663.

Snyder, C. and F. Zhang, 2003: Assimilation of simulated Doppler radar observations with an ensemble Kalman filter. *Mon. Wea. Rev.*, **131,** 1663-1677.

Sun, J. and N. A. Crook, 1997: Dynamical and microphysical retrieval from Doppler radar observations using a cloud model and its adjoint. Part I: Model development and simulated data experiments. *J. Atmos. Sci.*, **54,** 1642-1661.

Tao, W.-K. and J. Simpson, 1993: Goddard cumulus ensemble model. Part I: Model description. *Terres. Atmos. Ocean Sci.*, **4,** 35-72.

Tong, M. and M. Xue, 2005: Ensemble Kalman filter assimilation of Doppler radar data with a compressible nonhydrostatic model: OSSE Experiments. *Mon. Wea. Rev.*, **133**, 1789-1807.

Whitaker, J. S. and T. M. Hamill, 2002: Ensemble data assimilation without perturbed observations. *Mon. Wea. Rev.*, **130,** 1913-1924.

Wilson J. W., N. A. Crook, C. K. Mueller, J. Sun, and M. Dixon, 1998: Nowcasting thunerstorms: a status report. *Bull. Amer. Meteor. Soc.* **79**, 2079-2099.

Xue, M., K. K. Droegemeier, and V. Wong, 2000: The Advanced Regional Prediction System (ARPS)-A multiscale nonhydrostatic atmospheric simulation and prediction tool. Part I: Model dynamics and verification. *Meteor. Atmos. Physics*, **75,** 161-193.

Xue, M., D.-H. Wang, J. Gao, K. Brewster, and K. K. Droegemeier, 2003: The Advanced Regional Prediction System (ARPS), storm-scale numerical weather prediction and data assimilation. *Meteor. Atmos. Physics*, **82,** 139-170.

Xue, M., K. K. Droegemeier, V. Wong, A. Shapiro, K. Brewster, F. Carr, D. Weber, Y. Liu, and D.-H. Wang, 2001: The Advanced Regional Prediction System (ARPS) - A multiscale nonhydrostatic atmospheric simulation and prediction tool. Part II: Model physics and applications. *Meteor. Atmos. Phy.*, **76,** 143-165.

Xue, M., M. Tong, and K. K. Droegemeier, 2005: An OSSE framework based on the ensemble square-root Kalman filter for evaluating impact of data from radar networks on thunderstorm analysis and forecast. *J. Atmos. Ocean Tech.***,** Accepted.

Zhang, F., C. Snyder, and J. Sun, 2004: Impacts of initial estimate and observations on the convective-scale data assimilation with an ensemble Kalman filter. *Mon. Wea. Rev.*, **132,** 1238-1253.